Proc. Natl. Acad. Sci. USA
Vol. 94, pp. 4872–4877, May 1997
Biochemistry

Redesign of soluble fatty acid desaturases from plants for altered substrate specificity and double bond position

(unsaturated fatty acid/diiron/nonheme iron/rational design/protein engineering)

EDGAR B. CAHOON*, YLVA LINDQVIST†, GUNTER SCHNEIDER†, AND JOHN SHANKLIN*‡

*Biology Department, Brookhaven National Laboratory, Upton, NY 11973; and †Department of Medical Biochemistry and Biophysics, Karolinska Institute, Doktorsringen 4, S-171 77 Stockholm, Sweden

Communicated by Christopher R. Somerville, Carnegie Institution of Washington, Stanford, CA, March 13, 1997 (received for review January 31, 1997)

ABSTRACT **Acyl-acyl carrier protein (ACP) desaturases introduce double bonds at specific positions in fatty acids of defined chain lengths and are one of the major determinants of the monounsaturated fatty acid composition of vegetable oils. Mutagenesis studies were conducted to determine the structural basis for the substrate and double bond positional specificities displayed by acyl-ACP desaturases. By replacement of specific amino acid residues in a Δ^6-palmitoyl (16:0)-ACP desaturase with their equivalents from a Δ^9-stearoyl (18:0)-ACP desaturase, mutant enzymes were identified that have altered fatty acid chain-length specificities or that can insert double bonds into either the Δ^6 or Δ^9 positions of 16:0- and 18:0-ACP. Most notably, by replacement of five amino acids (A181T/A200F/S205N/L206T/G207A), the Δ^6-16:0-ACP desaturase was converted into an enzyme that functions principally as a Δ^9-18:0-ACP desaturase. Many of the determinants of fatty acid chain-length specificity in these mutants are found in residues that line the substrate binding channel as revealed by x-ray crystallography of the Δ^9-18:0-ACP desaturase. The crystallographic model of the active site is also consistent with the diverged activities associated with naturally occurring variant acyl-ACP desaturases. In addition, on the basis of the active-site model, a Δ^9-18:0-ACP desaturase was converted into an enzyme with substrate preference for 16:0-ACP by replacement of two residues (L118F/P179I). These results demonstrate the ability to rationally modify acyl-ACP desaturase activities through site-directed mutagenesis and represent a first step toward the design of acyl-ACP desaturases for the production of novel monounsaturated fatty acids in transgenic oilseed crops.**

Vegetable oils rich in monounsaturated fatty acids are important in human nutrition and can be used as renewable sources of industrial chemicals (1, 2). The ability to manipulate carbon chain lengths and double bond positions of monounsaturated fatty acids offers a way of altering the physical properties (e.g., melting points) and commercial uses of conventional plant oils (1, 2). In this regard, acyl-acyl carrier protein (ACP) desaturases are primary targets for the production of novel monounsaturated fatty acids in transgenic oilseed crops. Members of this family of soluble enzymes catalyze the insertion of a double bond into saturated fatty acids bound to ACP (3, 4). The most widely occurring of these enzymes is the Δ^9-stearoyl (18:0§)-ACP desaturase, which is associated with the synthesis of oleic acid (18:1Δ^9) in plants (5–9). In addition, several other acyl-ACP desaturases have been identified in specific tissues of a limited number of families or species of plants. These include a Δ^4-palmitoyl (16:0)-ACP desaturase of *Coriandrum sativum* (coriander) seed (10, 11), a Δ^6-16:0-ACP desaturase of *Thunbergia alata* (black-eyed Susan vine) seed (12), and a Δ^9-myristoyl (14:0)-ACP desaturase of *Pelargonium xhortorum* (geranium) trichomes (13). As their names indicate, these enzymes introduce double bonds into different positions (Δ^4, Δ^6, or Δ^9) of fatty acids of different chain lengths (14, 16, or 18 carbon atoms).

Despite their functional divergence, these enzymes share a high degree of amino acid sequence similarity (>70%) and, with the exception of short alignment gaps at their N and C termini, the primary structures of these enzymes are colinear. Thus, these desaturases almost certainly share a common structural fold and present an opportunity for understanding the molecular basis for chain-length recognition and positional placement of double bonds into fatty acids. In this report, we have addressed this question through the design of mutant enzymes based on amino acid sequence comparisons of acyl-ACP desaturases or on three-dimensional information from the recently reported crystal structure of the castor Δ^9-18:0-ACP desaturase (14). We demonstrate that the substrate and regio- specifities of acyl-ACP desaturases can be modified by the replacement of specific amino acid residues. We also show the utility of the crystal structure of the castor Δ^9-18:0-ACP desaturase in the interpretation of the fatty acid chain-length specificities of naturally occurring acyl-ACP desaturases and in the rational design of acyl-ACP desaturase activities.

MATERIALS AND METHODS

Preparation of Chimeric Enzymes and Site-Directed Mutants of the Δ^6-16:0-ACP Desaturase. Chimeric enzymes were prepared by linking portions of the coding sequence of the mature *T. alata* Δ^9-18:0- and Δ^6-16:0-ACP desaturases by means of native restriction enzyme sites or restriction sites generated by PCR. The coding sequences used were derived from the previously described cDNAs pTAD2 (15) and pTAD4 (12). Site-specific mutations in the coding sequence of amino acids 178–202 of the mature Δ^9-18:0-ACP desaturase (equivalent to residues 172–196 of the Δ^6-16:0-ACP desaturase) were introduced by extension and amplification of overlapping oligonucleotide primers using PCR with *Pfu* polymerase (Stratagene). As an example, mutations A188G/Y189F¶ were made with the following oligonucleotides (base changes are indicated by underlining): 5′-ATGGATCCTGGCACG-

The publication costs of this article were defrayed in part by page charge payment. This article must therefore be hereby marked "*advertisement*" in accordance with 18 U.S.C. §1734 solely to indicate this fact.

0027-8424/97/944872-6$2.00/0
PNAS is available online at **http://www.pnas.org**.

Abbreviation: ACP, acyl carrier protein.

‡To whom reprint requests should be addressed. e-mail: shanklin@bnl.gov.

§Fatty acid nomenclature: *x*:*y*, *x* is the number of carbon atoms in the fatty acid chain, and *y* is the number of double bonds. Δ^x indicates the position of the double bond relative to the carboxyl end of the fatty acid.

¶Unless otherwise indicated, amino acid numbering corresponds to the sequence of the mature castor Δ^9-18:0-ACP desaturase (see ref. 14).

GATAACAACCCGTAC-3′ (Primer 1); 5′-ACGAGGTG-TAGATAAATCCGAGGTACGGGTTGTTATCCG-3′ (primer 2); 5′-TATCTACACCTCGTATCAGGAGAGGGC-GACA-3′ (primer 3); and 5′-TTGAATTCCATGGGAAAT-CGCTGTCGCCCTCTCCTG-3′ (primer 4). PCRs were conducted without added template, using 12.5 pmol of primers 1 and 4 and 6.25 pmol of primers 2 and 3 in 50-μl reaction mixtures. For the first 10 PCR cycles, an annealing temperature of 37°C and an extension temperature of 72°C were used. This was followed by an additional 20 cycles with the annealing temperature increased to 55°C. Other mutations in the region of amino acids 178–202 were generated by using a similar combination of primers containing coding sequence of the wild-type enzyme or that of the desired mutation. PCR products were linked at their 5′ and 3′ ends to the coding sequence of amino acids 1–171 and 197–355 of the wild-type Δ^6-16:0-ACP desaturase by 5′ *Bam*HI and 3′ *Nco*I sites and assembled into the bacterial expression vector pET3d (Novagen). The mutation S205N/L206T/G207A was generated by PCR amplification of the coding sequence of amino acids 197–355 of the Δ^6-16:0-ACP desaturase, using as template a cDNA for this enzyme in pBluescript II SK (−) (Stratagene). The 5′ oligonucleotide (5′-TTTCCATGGGAACACG-GCTCGGCTAGCGAGGCAGAAGG-3′) contained the appropriate mutant codons (underlined), and the T7 primer was used as the 3′ oligonucleotide for PCRs. The amplification product was digested with *Nco*I and *Bcl*I and inserted into the *Nco*I/*Bam*HI site of pET3d. A *Nco*I/*Eco*RI fragment from this construct was then ligated to the coding sequence of amino acids 1–196 of wild-type or mutant Δ^6-16:0-ACP desaturases (e.g., A181T/A200F) to generate a full-length coding sequence. All PCR-generated DNA was sequenced using a Sequenase 2.0 kit (Amersham) to confirm the presence of desired mutations and the absence of any secondary mutations.

Preparation of Site-Directed Mutants of the Castor Δ^9-18:0-ACP Desaturase. Mutations L118F and P179I were introduced sequentially into the castor Δ^9-18:0-ACP desaturase. The mutation L118F was generated by overlap extension PCR (16) using the coding sequence of the mature wild-type castor Δ^9-18:0-ACP desaturase in the vector pET9d (Novagen) as the template. Two separate PCRs were conducted using the primer pairs (base changes are underlined): (*i*) T7 primer and 5′-CCGAACTCCATCGAAGGTATTCAGCA-3′ and (*ii*) 5′-TGCTGAATACCTTCGATGGAGTTCGG-3′ and 5′-GCAAAAGCCAAAACGGTACCATCAGGATCA-3′ (primer A). The agarose gel-purified products of the two reactions were combined and amplified together with the T7 primer and primer A. The product of this reaction containing the mutation for L118F was digested with *Xba*I and *Bam*HI and inserted in place of the corresponding portion of the wild-type castor Δ^9-18:0-ACP desaturase in the vector pET9d. The double mutant L118F/P179I was generated as described above using the coding sequence of the mutant L118F in pET9d as template and the primer pairs (base changes underlined): (*i*) T7 primer and 5′-GGACTGTTTTCTGTC-CGAATATCCATTCCTGAACCA-3′ and (*ii*) 5′-TGGT-TCAGGAATGGATATTCGGACAGAAAACAGTCC-3′ and primer A. The product generated following two rounds of PCR was digested with *Xba*I and *Pst*I and inserted in place of the corresponding portion of the wild-type castor Δ^9-18:0-ACP desaturase in vector pET9d.

Expression and Purification of Acyl-ACP Desaturases. Wild-type and mutant acyl-ACP desaturases were obtained by expression of the coding sequences in *Escherichia coli* BL21 (DE3) behind the T7 RNA polymerase promoter, using pET expression vectors (Novagen) as described above. Recombinant enzymes whose activities are described in Table 1 were purified from extracts of 6- to 9-liter bacterial cultures induced at 22°C (or at 30°C, in the case of the wild-type castor Δ^9-18:0-ACP desaturase and mutant L118F/P179I). Protein purification was performed using DEAE anion-exchange chromatography followed by perfusion cation-exchange chromatography using a 20 HS column (PerSeptive Biosystems). Mutant desaturases were obtained at 90% purity, and the wild-type Δ^6-16:0-ACP desaturase was recovered at approximately 80% purity as determined by SDS/PAGE with Coomassie blue staining. The wild-type castor Δ^9-18:0-ACP desaturase and mutant L118F/P179I were enriched to >90% purity by using only 20 HS perfusion cation-exchange chromatography. Following purification, enzymes were exchanged into a buffer consisting of 40 mM Tris·HCl (pH 7.5), 40 mM NaCl, and 10% (vol/vol) glycerol and stored in aliquots at −75°C.

Enzyme Assays. Acyl-ACP desaturation assays and analysis of reaction products were conducted as previously described (12) with the following modifications: recombinant *Anabaena* vegetative ferredoxin (22 μg per assay) and maize root ferredoxin:$NADP^+$ oxidoreductase (FNR) (0.4 unit per assay) were used in place of spinach ferredoxin and FNR, and concentrations of NADPH and [1-^{14}C]16:0- or 18:0-ACP per assay were increased to 2.5 mM and 1.2 μM, respectively. Acyl-ACPs were synthesized enzymatically using recombinant spinach ACP-I (17). Products and unreacted substrates were separated by argentation thin-layer chromatography (TLC) as methyl ester derivatives (11, 12, 18), and the distribution of radioactivity between these moieties was measured by phosphorimaging of TLC plates using IMAGEQUANT software (Molecular Dynamics) and by liquid scintillation counting of TLC scrapings.

Determination of Double Bond Positions. Double bond positions of monounsaturated fatty acid products were determined by the mobility of methyl ester derivatives on 15% argentation TLC plates (12, 18) and by gas chromatography–mass spectrometry (GC-MS) of dimethyl disulfide adducts of these derivatives (10, 12, 19). Desaturation assays for GC-MS analyses were conducted using radiolabeled 16:0- and 18:0-ACP and unlabeled 17:0-ACP as substrates for purified enzymes.

RESULTS AND DISCUSSION

Mutant Acyl-ACP Desaturases with Altered Activities. The studies described here were initiated prior to the availability of three-dimensional data from the crystal structure of the castor Δ^9-18:0-ACP desaturase (14). In the absence of this information, we attempted to understand the structural basis for differences in activities catalyzed by a Δ^6-16:0-ACP desaturase and a Δ^9-18:0-ACP desaturase by generating a series of chimeric enzymes that combined portions of these two desaturases (e.g., see Fig. 1). The activities of the resulting enzymes were then assessed to determine the effect on their substrate and regio-specificities. In this manner, a 30-amino acid domain encompassing residues 178–207 of the Δ^9-18:0-ACP desaturase was identified that contained determinants of both chain-

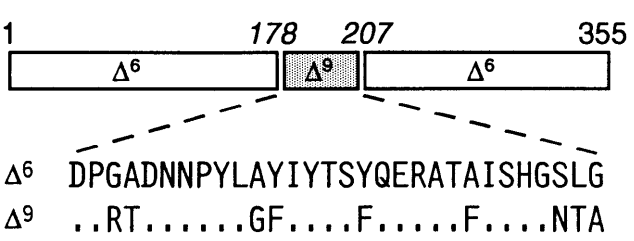

FIG. 1. Linear representation of chimera 1 and a sequence comparison of amino acids 178–207 of the mature Δ^6-16:0- (Δ^6) and Δ^9-18:0- (Δ^9) ACP desaturases from *T. alata* (refs. 12 and 15). Numbers in italics refer to amino acid positions in the mature Δ^9-18:0-ACP desaturase, and nonitalicized numbers indicate amino acid positions in the mature Δ^6-16:0-ACP desaturase.

length and double bond positional specificities. When this domain was introduced in place of the analogous portion of the Δ^6-16:0-ACP desaturase (Fig. 1), the resulting enzyme (designated chimera 1) displayed a mixture of Δ^6 and Δ^9 desaturase activities with 16:0- and 18:0-ACP (Table 1). In sharp contrast to the wild-type Δ^6-16:0-ACP desaturase, chimera 1 catalyzed Δ^6 and Δ^9 desaturation with 16:0-ACP at a ratio of 3:1 and with 18:0-ACP at a ratio of 1:1 (Table 1). In addition, the specific activity of chimera 1 with 18:0-ACP was twice that detected with 16:0-ACP (Table 1).

An additional novel activity was obtained using a smaller portion of the 30-amino acid domain described above. When residues 178–202 of the Δ^9-18:0-ACP desaturase were introduced in place of the corresponding portion of the Δ^6-16:0-ACP desaturase, an enzyme that functioned almost exclusively as a Δ^6 desaturase with 16:0- and 18:0-ACP was obtained (designated chimera 2; Table 1). The double bond positional specificity with 18:0-ACP was distinctly different than that of the wild-type Δ^6-16:0-ACP desaturase, which displayed mixed Δ^6 and Δ^9 desaturase activity with this substrate. In addition, chimera 2, unlike the wild-type enzyme, was almost equally active with 16:0- and 18:0-ACP (Table 1). Interestingly, the specific activity of chimera 2 with 16:0-ACP was 2-fold greater than that detected with the wild-type Δ^6-16:0-ACP desaturase. Also, the specific activity with 18:0-ACP was more than 15-fold greater than that displayed by the wild-type enzyme.

Amino acids 178–207 of the Δ^9-18:0-ACP desaturase contain nine residues that are different from those found in the equivalent portion of the Δ^6-16:0-ACP desaturase (Fig. 1). Through site-directed mutagenesis of the Δ^6-16:0-ACP desaturase, each of these residues, either individually or in combination, was converted to that present in the Δ^9-18:0-ACP desaturase. An activity qualitatively similar to that of chimera 1 was obtained by the following mutation of the Δ^6-16:0-ACP desaturase: A181T/A188G/Y189F/S205N/L206T/G207A (Fig. 2; Table 1). In addition, the chimera 2 phenotype (i.e., broadened fatty acid chain-length specificity) was achieved qualitatively by the mutation A188G/Y189F of the Δ^6-16:0-ACP desaturase (Fig. 2; Table 1).

Mutant desaturases with unexpected activities were also generated in these experiments. For example, the mutation A181T/A200F of the Δ^6-16:0-ACP desaturase gave rise to an enzyme that catalyzed primarily the Δ^9 desaturation of 18:0-ACP, but functioned as a Δ^6 desaturase with 16:0-ACP (Table 1). Furthermore, the mutation A181T/A200F/S205N/L206T/G207A of the Δ^6-16:0-ACP desaturase yielded an enzyme that functioned primarily as a Δ^9-18:0-ACP desaturase. This enzyme displayed only Δ^9 desaturase activity with 18:0-ACP and was nearly 4-fold more active with this substrate than with 16:0-ACP (Fig. 2; Table 1). However, like mutant A181T/A200F, this enzyme retained Δ^6 desaturase activity with 16:0-ACP.

Of note, the enzyme assay used in these studies precluded the collection of large amounts of kinetic data. However, K_m values determined for the wild-type Δ^6-16:0- ACP desaturase, chimera 2, and mutant A188G/Y189F were in the range of 0.2 to 0.6 μM with both 16:0- and 18:0-ACP, suggesting that, at least in the case of these enzymes, changes in the substrate binding properties can be discounted as an underlying cause of differences in activities.

Interpretation of Mutant Enzymes in Terms of the Crystal Structure of the Δ^9-18:0-ACP Desaturase. Recently, the crystal structure of castor Δ^9-18:0-ACP desaturase was determined (14), making it possible to interpret a portion of the above results in terms of the arrangement of the active site. The subunit structure of the Δ^9-18:0-ACP desaturase contains a catalytic diiron cluster, which represents a fixed point for the introduction of the double bond (14) (Fig. 3). Adjacent to the iron atoms is a deep and narrow channel that likely represents the binding pocket for the stearic acid (18:0) portion of the substrate. The channel imposes a bent conformation on the fatty acid chain between carbon atoms 9 and 10, the site of desaturation. This conformation corresponds to the *cis* configuration of the oleoyl (18:1Δ^9)-ACP product and positions the location of double bond insertion close to the diiron center. In this model, the architecture of the fatty acid binding channel in relation to the catalytic iron cluster affects both substrate specificity and the position at which double bonds are introduced.

With regard to substrate specificity of acyl-ACP desaturases, the geometry of the lower portion of the binding pocket places severe constraints on the length of the acyl chain that can be

Table 1. Specific activities of wild-type and mutant Δ^6-16:0-ACP desaturases with 16:0- or 18:0-ACP

	Specific activity, nmol/min per mg protein				Ratio of total specific activity
	16:0-ACP		18:0-ACP		
Enzyme*	Δ^6	Δ^9	Δ^6	Δ^9	16:0-ACP:18:0-ACP
Δ^6-16:0-ACP desaturase (wild type)	100 ± 3	ND	11 ± 1 (2:1)	5.5 ± 0.2	6:1
Chimera 1 ($\Delta^6/\Delta^9_{178\text{-}207}/\Delta^6$)	13 (3:1)	4.0	15 (1:1)	17	1:2
Chimera 2 ($\Delta^6/\Delta^9_{178\text{-}202}/\Delta^6$)	227 ± 25	ND	253 ± 25 (50:1)	5.3 ± 0.5	1:1
A181T/A188G/Y189F/S205N/L206T/G207A	33 ± 4 (3:1)	12 ± 1	31 ± 2 (1:2)	53 ± 5	1:2
A188G/Y189F	34 ± 3	ND	34 ± 4 (50:1)	0.7 ± 0.1	1:1
A181T/A200F	149	ND	3.1 (1:15)	44	3:1
A181T/A200F/S205N/L206T/G207A	19 ± 1 (14:1)	1.4 ± 0.3	ND	76 ± 5	1:4

Shown are Δ^6 and Δ^9 desaturase activities with each substrate ± SD of three independent measurements. ND, not detected. The numbers in parentheses are the ratio of Δ^6:Δ^9 activity with the given substrate. In addition to results presented in this table, approximately 15% of the desaturation products formed by the reaction of 17:0-ACP with the wild-type Δ^6-16:0-ACP desaturase was detected by GC–MS as the 17:1 Δ^7 isomer. The remainder of the product was 17:1Δ^6 with trace amounts of 17:1Δ^9 also detected. Small amounts of Δ^7 isomers were also present in mass spectra of products formed from 16:0- and 18:0-ACP with the wild-type Δ^6-16:0-ACP desaturase and several of the mutants. These accounted for <5% of the total products. No Δ^8 isomers were detected in mass spectra of desaturation products.

*Amino acid numbering corresponds to the sequence of the mature Δ^9-18:0-ACP desaturase.

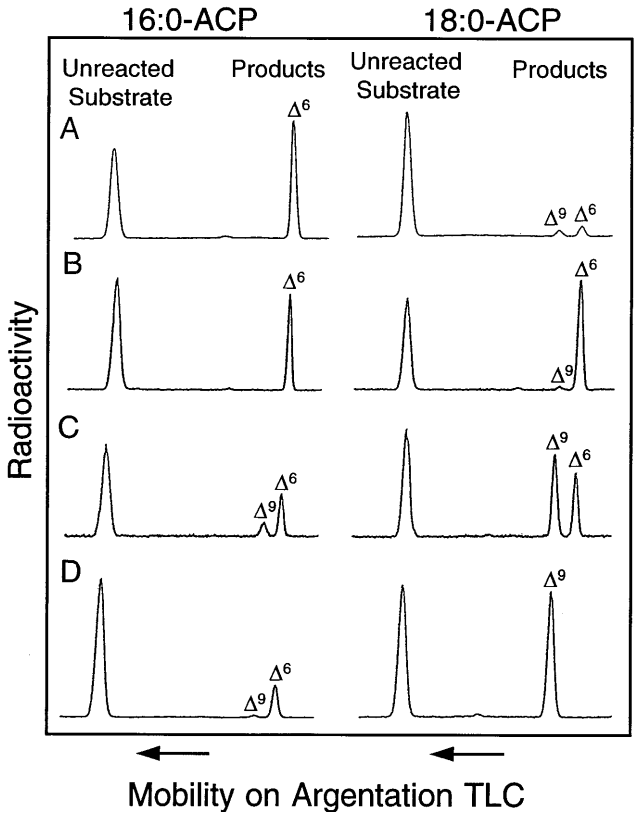

FIG. 2. Comparison of the relative activities of the wild-type Δ^6-16:0-ACP desaturase and mutant forms of this enzyme. Shown are monounsaturated products (e.g., 16:1 or 18:1) and unreacted substrate from reactions conducted with the wild-type Δ^6-16:0-ACP desaturase (*A*) and mutants A188G/Y189F (*B*), A181T/A177G/Y189F/S205N/L206T/G207A (*C*), and A181T/A200F/S205N/L206T/G207A (*D*) using [1-^{14}C]16:0- or [1-^{14}C]18:0-ACP as substrate. Assays with each enzyme were conducted for equal periods of time using equivalent concentrations of enzyme and substrate. As shown, methyl ester derivatives of products and unreacted substrates were separated by argentation thin-layer chromatography (TLC), and radioactivity was detected by phosphorimaging. Double bond positions were confirmed by GC-MS analyses of dimethyl disulfide adducts of fatty acid methyl esters.

accommodated beyond the point where the double bond is to be introduced (Fig. 3). As such, residues at the bottom of the substrate channel are likely the most critical for determining fatty acid chain-length specificity. This explains the functional properties of chimera 2 and mutant A188G/Y189F which display increased Δ^6 desaturase activity with 18:0-ACP compared with the wild-type Δ^6-16:0-ACP desaturase. Based on the model of the active site, substitution of alanine-188 for a smaller glycine and tyrosine-189 for phenylalanine extends the cavity at the bottom of the active site enough to accommodate the two additional carbon atoms at the methyl end of 18:0-ACP (Fig. 3). As a result, chimera 2 and mutant A188G/Y189F are able to desaturate 18:0-ACP with a rate comparable to that observed with 16:0-ACP.

More difficult to interpret are alterations in the double bond positional specificities of mutants described above. This class of fatty acid desaturases inserts a double bonds at a characteristic position from the carboxyl end of acyl chains (11, 20). Thus, the site of double bond insertion by acyl-ACP desaturases is likely associated with interactions between the upper part of the active site and the ACP portion of substrates. Assuming that ACP binds in the same manner in all acyl-ACP desaturases, differences in the amino acid side chains at the enzyme surface and/or those lining the upper portion of the substrate binding channel would allow the enzyme to accom-

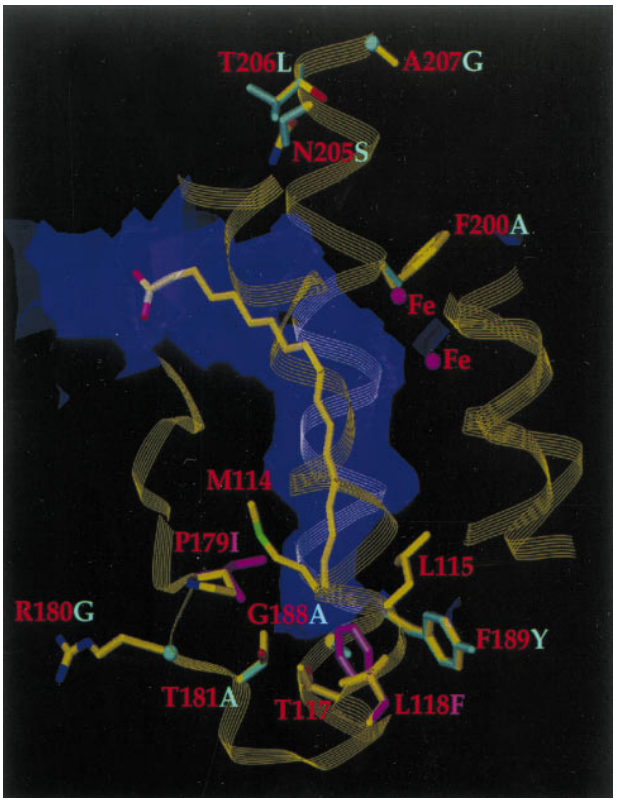

FIG. 3. Schematic view of the substrate channel of the Δ^9-18:0-ACP desaturase. A model of the stearic acid (18:0) substrate is fitted in the binding pocket of the Δ^9-18:0-ACP desaturase, and amino acid side chains important in fatty acid chain-length specificity are shown as stick models (with red labels). Residues that have been replaced in mutants of the Δ^6-16:0-ACP desaturase are indicated in cyan, and mutant L118F/P179I is shown in magenta.

modate different lengths of the fatty acid chain between the site of double bond insertion and the thioester linkage to ACP. However, in the absence of a crystal structure of the desaturase that includes a bound acyl-ACP substrate, it is not possible to interpret differences in double bond positional specifities of the mutants described above or in naturally occurring enzymes such as the Δ^4- and the Δ^6-16:0-ACP desaturases. Of the residues that contribute to altered double bond positional specificity in the mutants described above, alanine-200 is on the surface pointing away from the substrate channel and amino acids 205–207 are located outside of the active site (Fig. 3). It is possible that these residues mediate changes in activity by means of subtle packing effects in the enzyme rather than through direct interactions with substrates, as has been reported for mutants of serine proteases with altered function (21, 22).

Modeling of the Active Sites of Variant Acyl-ACP Desaturases. The crystallographic model of the active site of the castor Δ^9-18:0-ACP desaturase also provides useful information regarding the fatty acid chain-length specifities of naturally occurring variant acyl-ACP desaturases (e.g., the Δ^9-14:0-, Δ^4-16:0-, and Δ^6-16:0-ACP desaturases). As shown in Fig. 4, variant desaturases that accept substrates with fewer carbon atoms in the distal portion of the active site (i.e., the region beyond the site of double insertion) have their binding clefts occluded by substitutions of amino acids with bulkier side chains. The amino acids involved in determining the specificity in this part of the binding site are as follows: 114–115, 117–118, 179, 181, and 188–189. For example, the Δ^9-18:0-ACP desaturase, which accepts nine carbon atoms of the fatty acid substrate beyond the point of double bond insertion, contains a methionine, proline, and glycine at amino acid positions 114,

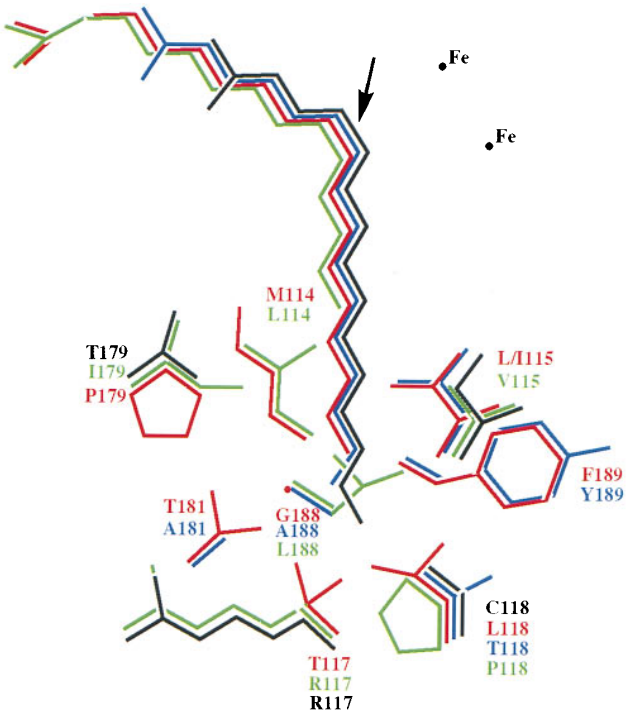

FIG. 4. A model of fatty acids bound in the active site of enzymes in the family of soluble acyl-ACP-desaturases. The color code is red, Δ^9-18:0-ACP desaturase from castor and *T. alata*; blue, Δ^6-16:0-ACP desaturase from *T. alata*; green, Δ^9-14:0-ACP desaturase from geranium; and black, Δ^4-16:0-ACP desaturase from coriander. The position of the catalytic diiron center is indicated, and an arrow shows the position of double bond insertion into fatty acid substrates (shown as stick figures). Amino acid numbering is given with respect to the sequence of the mature castor Δ^9-18:0-ACP desaturase. As indicated, amino acid side chains that line the channel are typically smaller in enzymes with substrates that have a longer portion of the fatty acid chain beyond the site of double bond insertion.

179, and 188, respectively. In contrast, the Δ^9-14:0-ACP desaturase, which accepts five carbon atoms of the substrate in the deep portion of the active site, contains the larger hydrophobic residues leucine, isoleucine, and leucine at positions 114, 179, and 188, respectively, (Fig. 4). Such amino acid differences likely contribute to a smaller binding pocket in the Δ^9-14:0-ACP desaturase relative to the Δ^9-18:0-ACP desaturase.

Rational Design of Acyl-ACP Desaturase Activities. Residues described above and shown in Fig. 4 that line the lower portion of the active site represent potential targets for the rational design of acyl-ACP desaturase activities with respect to fatty acid chain-length specificity. As a test of this, leucine-118 and proline-179 of the mature castor Δ^9-18:0-ACP desaturase were replaced with the bulkier residues phenylalanine and isoleucine, respectively (Fig. 3). Consistent with our model of the active site, these substitutions yielded an enzyme that was functionally converted from a Δ^9-18:0-ACP desaturase to a Δ^9-16:0-ACP desaturase (Fig. 5). The altered activity resulted both from a reduction in the specific activity with 18:0-ACP and an increase in the specific activity with 16:0-ACP. Overall, the specific activity of the L118F/P179I mutant with 16:0-ACP was more than 15-fold greater than that displayed by the wild-type Δ^9-18:0-ACP desaturase with this substrate. GC-MS analyses of desaturation products indicated that the Δ^9 position was the exclusive site of double bond insertion when the mutant was presented with 16:0-ACP. However, when 18:0-ACP was provided as a substrate, not only was 18:1Δ^9 formed, but approximately 5% of the desaturation products were detected as the Δ^{10} isomer. This is consistent with a reduced

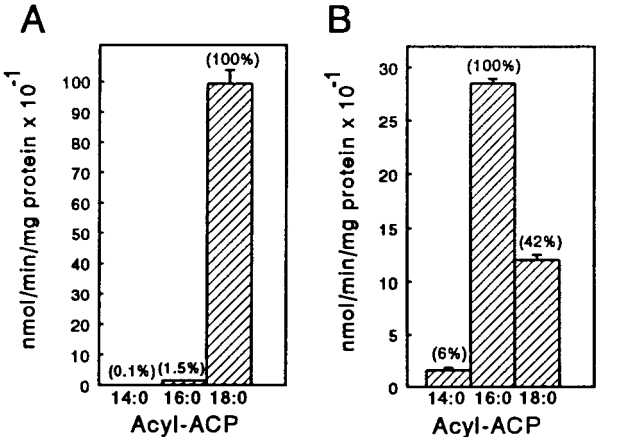

FIG. 5. Comparison of the specific activities of the wild-type castor Δ^9-18:0-ACP desaturase (*A*) and the mutant L118F/P179I (*B*) with acyl-ACP substrates of different chain lengths. The numbers in parenthesis indicate the relative activity of each enzyme with 14:0-, 16:0-, and 18:0-ACP. Specific activity values are the means from three or four independent assays ± SD.

ability of the binding pocket of the L118F/P179I mutant to accommodate the longer acyl chain of the 18:0-ACP substrate.

Overall, these results demonstrate the ability to modify the substrate and double bond positional specificities of acyl-ACP desaturases by using amino acid sequence alignments either alone or in conjunction with three-dimensional structural data from the castor Δ^9-18:0-ACP desaturase (14). These two approaches provided unique and complementary information with regard to understanding the molecular mechanisms of the substrate and regio-specificities displayed by acyl-ACP desaturases. In addition, several of the mutants described here have possible biotechnological applications. For example, chimera 2 or the Δ^6-16:0-ACP desaturase mutant A188G/Y189F may provide a means of producing petroselinic acid (18:1Δ^6) in transgenic crop plants. This fatty acid has potential use in the production of low-caloric margarine and as a precursor of adipic acid for the manufacture of nylon 66 (1, 2). Also, the rationally designed L118F/P179I mutant of the castor Δ^9-18:0-ACP desaturase may be useful in enhancing the unsaturated fatty acid quality of vegetable oils through the reduction of palmitic acid (16:0) content. These results along with additional information from crystallographic studies of acyl-ACP desaturases will likely lead to the continued design of enzymes for the production of novel monounsaturated fatty acids in transgenic oilseed crops.

We thank J. Ohlrogge and N. Engeseth for assistance with GC–MS analyses and V. Ramakrishnan and K. Schmid for helpful suggestions. We also thank Office of Basic Energy Sciences of the U.S. Department of Energy for support of E.B.C. and J.S. and the Swedish Natural Science Research Council for support to Y.L.

1. Murphy, D. J. (1992) *Trends Biotechnol.* **10,** 84–87.
2. Ohlrogge, J. B. (1994) *Plant Physiol.* **104,** 821–826.
3. Heinz, E. (1993) in *Lipid Metabolism in Plants*, ed. Moore, T. S. (CRC, Boca Raton, FL), pp. 33–89.
4. Ohlrogge, J. & Browse, J. (1995) *Plant Cell* **7,** 957–970.
5. Nagai, J. & Bloch, K. (1968) *J. Biol. Chem.* **243,** 4626–4633.
6. Jaworski, J. G. & Stumpf, P. K. (1974) *Arch. Biochem. Biophys.* **162,** 158–165.
7. McKeon, T. A. & Stumpf, P. K. (1982) *J. Biol. Chem.* **257,** 12141–12147.
8. Shanklin, J. & Somerville, C. (1991) *Proc. Natl. Acad. Sci. USA* **88,** 2510–2514.
9. Thompson, G. A., Scherer, D. E., Foxall-Van Aken, S., Kenny, J. W., Young, H. L., Shintani, D. K., Kridl, J. C. & Knauf, V. C. (1991) *Proc. Natl. Acad. Sci. USA* **88,** 2578–2582.

10. Cahoon, E. B., Shanklin, J. & Ohlrogge, J. B. (1992) *Proc. Natl. Acad. Sci. USA* **89,** 11184–11188.
11. Cahoon, E. B. & Ohlrogge, J. B. (1994) *Plant Physiol.* **104,** 827–844.
12. Cahoon, E. B., Cranmer, A. M., Shanklin, J. & Ohlrogge, J. B. (1994) *J. Biol. Chem.* **269,** 27519–27526.
13. Schultz, D. J., Cahoon, E. B., Shanklin, J., Craig, R., Cox-Foster, D. L., Mumma, R. O. & Medford, J. I. (1996) *Proc. Natl. Acad. Sci. USA* **93,** 8771–8775.
14. Lindqvist, Y., Huang, W., Schneider, G. & Shanklin, J. (1996) *EMBO J.* **15,** 4081–4092.
15. Cahoon, E. B., Becker, C. K., Shanklin, J. & Ohlrogge, J. B. (1994) *Plant Physiol.* **106,** 807–808.
16. Ho, S. N., Hunt, H. D., Horton, R. M., Pullen, J. K. & Pease, L. R. (1989) *Gene* **77,** 51–59.
17. Rock, C. O. & Garwin, J. L. (1979) *J. Biol. Chem.* **254,** 7123–7128.
18. Morris, L. J., Wharry, D. M. & Hammond, E. W. (1967) *J. Chromatography* **31,** 69–76.
19. Yamamoto, K., Shibahara, A., Nakayama, T. & Kajimoto, G. (1991) *Chem. Phys. Lipids* **60,** 39–50.
20. Gibson, K. J. (1993) *Biochim. Biophys. Acta* **1169,** 231–235.
21. Hedstrom, L. (1994) *Curr. Opin. Struct. Biol.* **4,** 608–611.
22. Schellenberger, V., Turck, C. W., Hedstrom, L. & Ritter, W. J. (1993) *Biochemistry* **32,** 4349–4353.